Effect of cryogenic assistance on hole shrinkage during Ti6Al4V drilling

Johan Merzouki[1,2] · Gérard Poulachon[1] · Frédéric Rossi[1] · Yessine Ayed[3] · Guillaume Abrivard[2]

Abstract
This paper focuses on the impact of cryogenic assistance on the drilling of Ti6Al4V titanium alloy. It develops a relation between the phenomenon of hole shrinkage and measurements performed either during or after the machining operation. Indeed, because this phenomenon is apparently strongly associated with heat generation, which is the main issue in titanium alloy drilling, this work proposes to verify the effect of liquid nitrogen cooling on hole shrinkage, quantify it, and then relate it to these measurements. Specifically, the cutting forces and final hole geometry are analyzed and their variations are explained using the collected data on hole shrinkage.

Keywords Drilling · Cryogenic assistance · Liquid nitrogen · Hole shrinkage · Cutting forces · Hole geometry

1 Introduction

Despite being known since several decades, the Ti6Al4V titanium alloy is still significant in engineering design, notably in the biomedical and aeronautic industries. As stated by Donachie [1], owing to their properties of remarkable strength to weight ratio and outstanding corrosion resistance, which are maintained even at elevated temperatures, titanium alloys are good candidates for high-performance applications.

Although widely used, Ti6Al4V is considered to be a difficult-to-machine material owing to its poor thermal diffusivity, which leads to heat evacuation issues. Indeed, Ghani et al. [2] found that the rapid temperature increases that occur when machining titanium alloys led to the adhesion of a Ti layer on the cutting edges of the carbide tools. In some cases, this unwanted additional layer was considered to be responsible for brittle fracture because it induced stress concentration on the edges. Moreover, Ramirez et al. [3] demonstrated the occurrence of a diffusion of elements from the tool to the work material when the temperature at the cutting interface was increased, weakening the tool in a progressive manner. In the case of drilling, Cantero et al. [4] identified both these wear mechanisms on the edges as well as margins of the used carbide drills. In addition, their study on the hole quality and surface integrity leads to the conclusion that heat may be responsible for the undesirable microstructural changes that occurred near the machined surface. Furthermore, the burr height was strongly associated with the intensity of the temperature reached in the cutting zone. Dornfeld et al. [5] reached the same conclusion concerning the burr height in Ti6Al4V drilling, confirming the importance of the thermal aspect in this regard. Furthermore, Kalidas et al. [6] established a relation between the roughness of the surface and elevation of temperature and showed that the hole quality was superior when heating was limited.

Considering the previous assessments, the origination of the concept of cryogenically assisted Ti6Al4V machining is understandable. Indeed, replacing the usual approach of cooling and lubrication by liquid nitrogen to cool down the cutting area was considered as a potential method for improving tool life by managing the heat issues. Therefore, the concept was tested by several researchers, such as Hong and Ding [7] whose study showed that cryogenic assistance applied to the turning of Ti6Al4V allowed a better tool life as well as lower temperatures in the cutting zone in comparison with dry machining. Dhananchezian and Kumar [8] compared the

✉ Frédéric Rossi
frederic.rossi@ensam.eu

[1] Arts et Metiers Institute of Technology, LaBoMaP, HESAM Université, 71250 Cluny, France

[2] Airbus Central Research and Technology—Technocampus Composites, Chemin du Chaffault, 44340 Bouguenais, France

[3] Arts et Metiers Institute of Technology, LAMPA, 2 Boulevard du Ronceray, 49035 Angers, France

https://doi.org/10.1007/s00170-020-05381-z

classical emulsion lubrication with cryogenic assistance in Ti6Al4V turning and observed the same tendencies as above, which were subsequently also confirmed by the minimum quantity lubrication (MQL) study by Kaynak et al. [9] on the turning of the Ti-5553 alloy. Venugopal et al. [10] further analyzed the effect of cryogenic assistance on the wear mechanisms and concluded that the cooling allowed to limit the diffusion phenomenon in Ti6Al4V turning, thus explaining the improved tool life.

Several other potential benefits of using cryogenic assistance were studied. For instance, Rotella et al. [11] compared the surface integrity in dry cutting, MQL, and cryogenic-assistance conditions and observed an improvement in the surface roughness and hardness as well as a reduction in the chemical phase changes when cryogenic cooling was applied. Kim et al. [12] also noticed an improvement in surface roughness and occurrence of phase changes when cryogenic assistance was used in Ti6Al4V turning. Concerning residual stresses, no studies were found for titanium alloy machining, but Pu et al. [13] have reported that it led to advantageous compressive residual stresses in the case of AZ31B Mg alloy. The same conclusions were reached for Inconel 718 and AISI 52100 steel by Pusavec et al. [14] and Biček et al. [15], respectively. Although some tendencies seem to have been verified, there are other effects that are still unclear. Concerning the cutting forces, the state-of-the-art provides mixed results because researchers such as Hong et al. [16] found that they increased, whereas others such as Bermingham et al. [17] reported that they decreased.

Finally, considering the lack of scientific results concerning the impact of cryogenic assistance on the drilling of Ti6Al4V, this work aims at investigating some of these effects. Moreover, an innovative approach is proposed because this study focuses on the phenomenon of hole shrinkage that occurs during the drilling of titanium alloys and is suspected to be strongly associated with heat generation. Indeed, as illustrated in Fig. 1 and stated by Merzouki et al. [18], the drilled hole has a smaller diameter than the diameter of the drill that is expected to be machined. Because a drill is slightly conical, the shrinkage of the hole on the tool leads to a contact whose height is proportional to the resulting diameter difference. Therefore, two types of mechanical loads are generated by this phenomenon:

- Tangential loads caused by the friction between the margins of the drill and machined hole, which are also responsible for heat generation. The resulting torque can easily be measured by using equipment such as rotating dynamometers.
- Radial loads caused by the contraction of the hole on the margins. Because the usual approaches do not allow to measure them, Merzouki et al. [18] proposed a method to determine them.

In the scientific literature, discussions of parameters affecting hole shrinkage are available. Authors like Yagishita and Morita [19] give metallurgical explanations showing that drilling temperature in Ti6Al4V is increasing the amount of β phase in the hole subsurface, leading to a smaller diameter. With similar conditions, Li et al. [20] demonstrate that the high strain and high strain rate associated with temperature can lead to β to α phase transformation.

For example, Bono and Ni [21] used a model in which the thermal expansion of the tool and contraction of the test sample were determined in an attempt to predict the hole geometry in the case of aluminum alloy drilling. Bonnet [22] established that two types of elastic deformations occurred once the edges of the drill had passed: the first being the elastic spring back following the unloading of the hole surface, and the second, the strain caused by the thermal loads induced by the operation. In addition, Nobre and Outeiro [23] used a hybrid numerical–experimental method to determine the residual

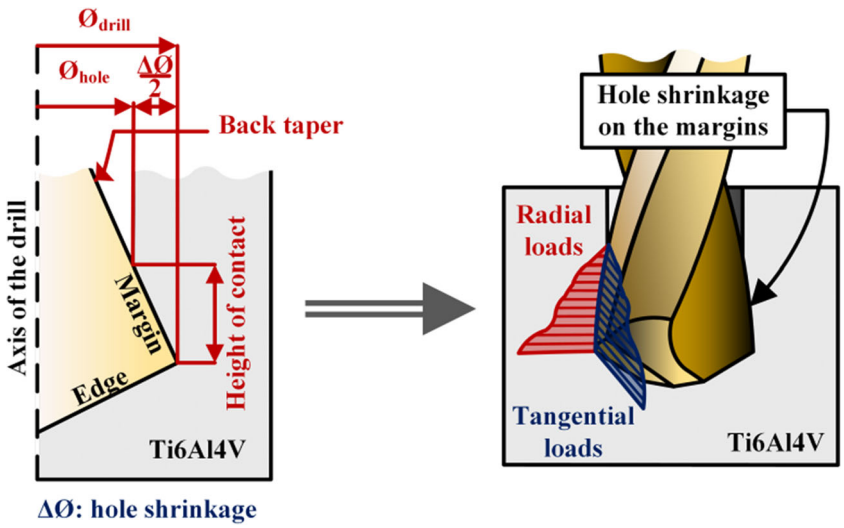

Fig. 1 Mechanical loads induced by the hole shrinkage on the margins [18]

strains and stresses induced by the drilling of titanium alloys. Using these results, they could calculate the strain relaxation occurring after the drilling, which was responsible for the diameter changes of the hole.

Therefore, this work proposes to verify the effect of cryogenic assistance on the phenomenon of hole shrinkage and relate this impact to the measured forces and hole dimensions under both dry-cutting and cryogenic-assistance conditions.

2 Experimental setup

2.1 Phase 1: variation in cutting parameters

Figure 2 shows the experimental setup with a three-axis HURON KX10 CNC milling center used to perform the drillings. Cutting tools are composed of ISCAR removable carbide heads (reference ICM 120 IC908) and a SUMOCHAM holder (reference DCN 120-060-16-5D). Their main geometrical specifications were a 12 mm diameter $Ø_{head}$ with a k7 tolerance ($12.001 < Ø_{head} < 12.019$), 1% back taper angle, and 140° tool tip angle. Two Ti6Al4V plates were drilled, one for the dry-cutting condition and the other for the cryogenic assistance. These samples were 25.5 mm thick and 54 holes were drilled on each of them. The liquid nitrogen used to implement the cryogenic assistance was stored in a tank with an internal pressure of 10 bar. The cryogenic fluid was driven to the cutting zone through the spindle and internal lubricant holes of the tool.

The objective of this experiment was to determine the effects of cryogenic assistance on Ti6Al4V drilling in comparison with the dry-cutting condition. Nine sets of cutting speeds (V_c) and feeds (f) were tested for both. The used cutting parameters are summarized in Table 1. Four indexable heads were used, two with dry cutting and two with cryogenic assistance. Each tool tip was used to drill 27 holes, repeating each of the nine sets of cutting parameters thrice for a total of $2 \times 9 \times 3 = 54$ holes, implying that each couple was tested six times for both cryogenic and dry-cutting conditions. An interval of 2 min was kept between each hole to avoid heat accumulation.

Feed force F_z and torque M_z were measured using a KISTLER dynamometer type 9255B. Figure 3 presents the details of the data treatment. Particularly, it shows that knowing the geometrical parameters of the tool, drilled depth can be used to verify when the tool is fully engaged (between Z_2 and Z_3) and compute the mean values of torque $M_{z\ mean}$ and feed force $F_{z\ mean}$. It also displays that by analyzing the exit of the drill, $M_{z\ mean}$ can be decomposed into torque contributions from the edges, margins, and chips, respectively, i.e., $M_{z\ edges}$, $M_{z\ margins}$, and $M_{z\ chips}$. Finally, it explains that height of contact H between the margins and hole walls is determined by identifying the instant when the torque due to the friction returns to zero, implying that the contact has ended.

The hole dimensions were measured using a Sentronics i-Dex-tf device. Figure 4 describes the measurements made and subsequently presented. Particularly, it shows that the shape reconstitutions that will be presented are built from 15 diameter measurements performed on the height of the drilled holes. It also explains that diameter of the inscribed cylinder $Ø_{ins}$ corresponds to the diameter of the maximum-sized perfect cylinder that could be inserted in the measured hole. Finally, it clarifies the measurement of cylindricity, which is the distance between the two coaxial cylinders containing the measured surface.

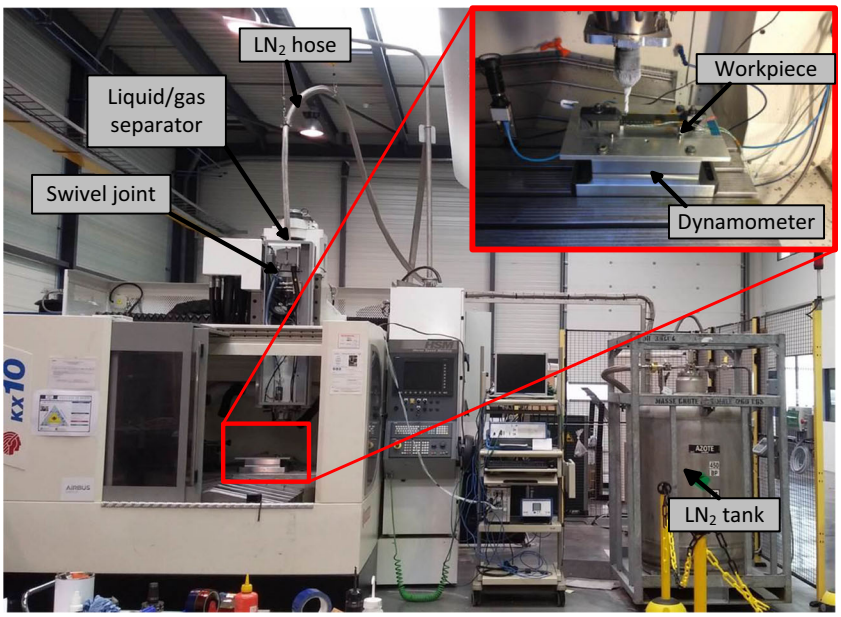

Fig. 2 Experiment setup with LN_2 feed through the tool

Table 1 Tested cutting parameters V_c and f

Tested cutting parameters			
Feed f (mm/rev)	0.08	0.16	0.24
Cutting speed V_c (m/min)	15	30	45

2.2 Phase 2: wear tests

In the second phase, wear tests were performed with the same CNC milling center, cutting tools, and cryogenic setup. The drilled Ti6Al4V plates were 25.5 mm thick. The holes were machined with a unique set of cutting parameters ($V_c = 15$ m/min, $f = 0.08$ mm/rev). To amplify the thermal issues and approach a production pacing, a break of 10 s was allowed between each drilling operation. The aim of these tests was to determine the effect of tool wear on the hole shrinkage, cutting forces, and hole dimensions under both dry-cutting and cryogenic conditions.

3 Results and discussion

Before discussing the results, it should be noted that all the displayed error bars have a length equal to the standard deviation and are centered on the mean value.

3.1 Phase 1: variation in cutting parameters

3.1.1 Height of contact *H* between the margins and hole

The back spring of the hole on the drill can be quantified by the height of contact H as shown on Fig. 3 and is due both to the high elasticity of titanium and the thermal expansion of the surface. On Fig. 3, H is determined by the length between the output of the tool edges of the sample (measured by Z CNC axis feedback) and the position when M_z is back to a null value (end of contact between the tool chisel and the hole). Figure 5 shows sequentially the results concerning height of contact H during the drilling as a function of cutting speed V_c and feed f.

With or without cryogenic assistance, the effect of the cutting speed is unclear, particularly because the extracted values of H are quite scattered when $V_c = 15$ m/min for the dry-cutting condition. The dispersion (here calculated with the square root) of the values of the height of contact for cryogenic conditions is the third of the values for dry conditions. It can be explained by the thermomechanical instability: hole shrinkage induces a friction heat source which induces a surface thermal dilatation which leads to more shrinkage …. This phenomenon is stabilized by the LN_2 cooling down.

The results show a clear tendency of the height of contact to increase with the feed. Regardless of the chosen cutting parameters, the height of contact remains significantly higher for

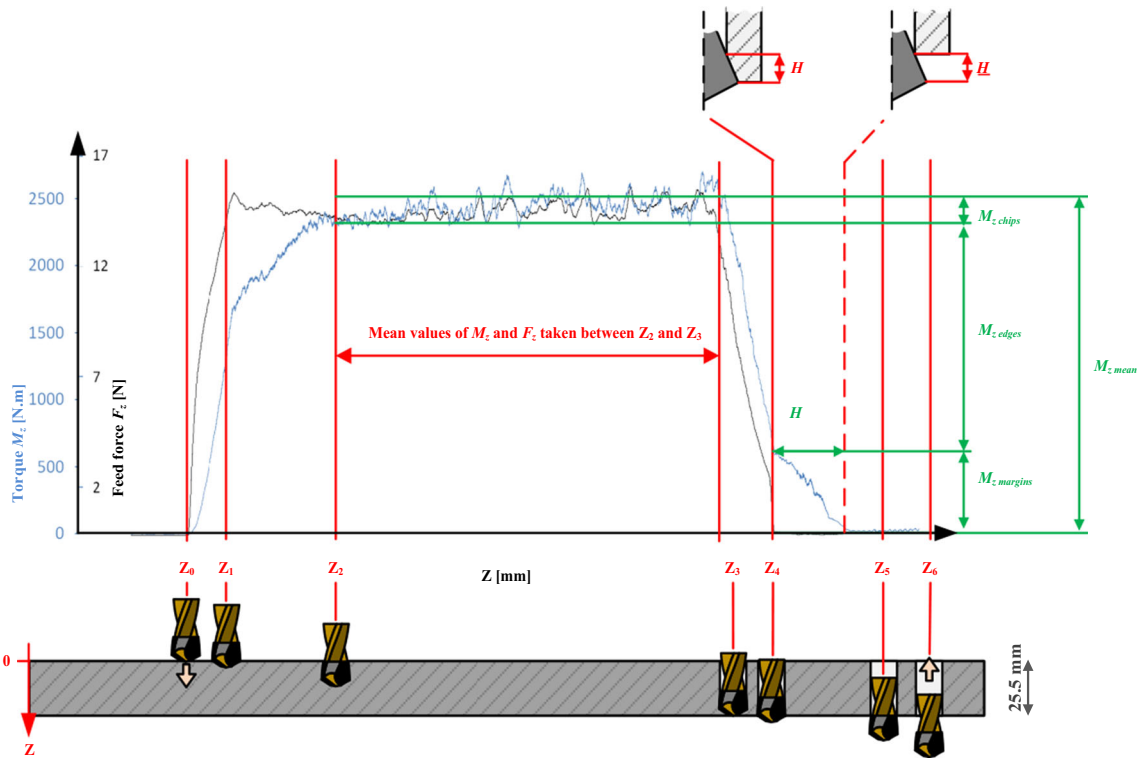

Fig. 3 Description of the various drilling steps ($V_c = 30$ m/min, $f = 0.24$ mm/rev, dry conditions)

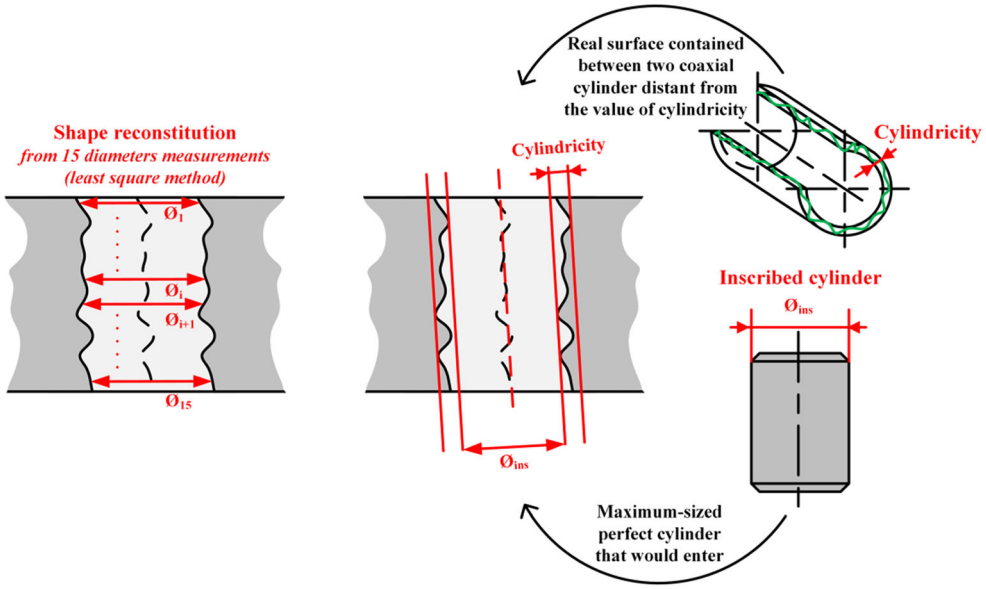

Fig. 4 Hole geometry measurements using the Sentronics i-Dex-tf device

the dry-cutting condition because the mean values are 2.5 to 5.5 times larger than with cryogenic assistance. Consequently, it demonstrates that LN_2 cooling allows to limit the hole shrinkage and confirms the major role of surface thermal dilatation in this phenomenon.

3.1.2 Evolution of mean feed force $F_{z\ mean}$

Figure 6 shows sequentially the mean values of feed force $F_{z\ mean}$ (measurement explained in Fig. 3) during the drilling as a function of cutting speed V_c and feed f.

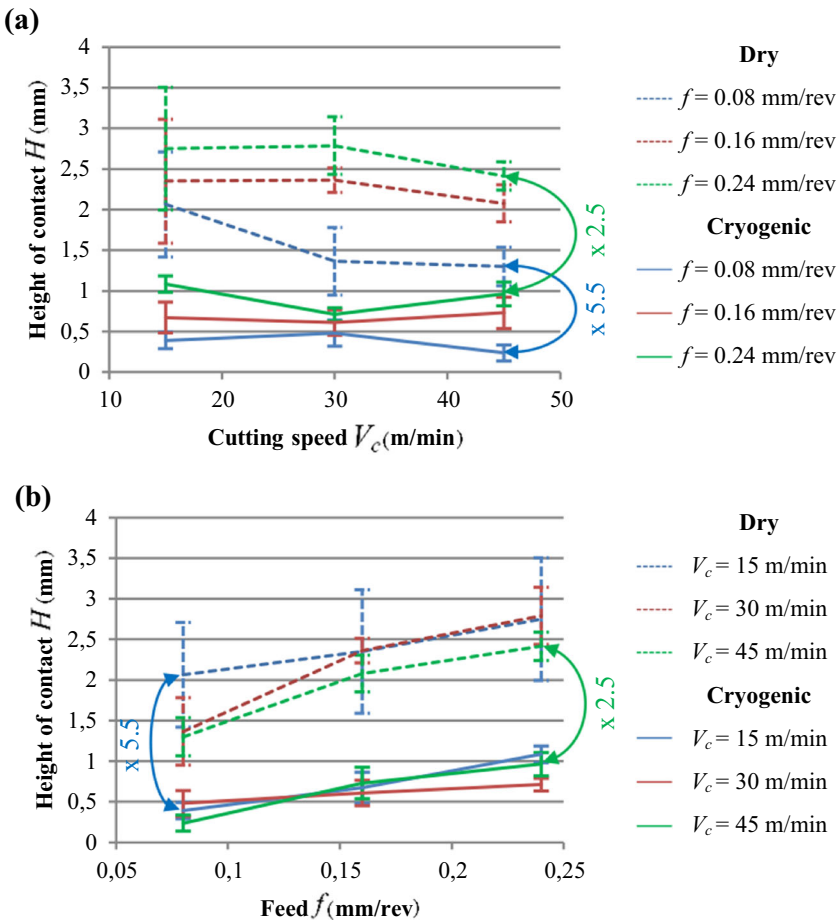

Fig. 5 Height of contact H as a function of (a) cutting speed V_c and (b) feed f

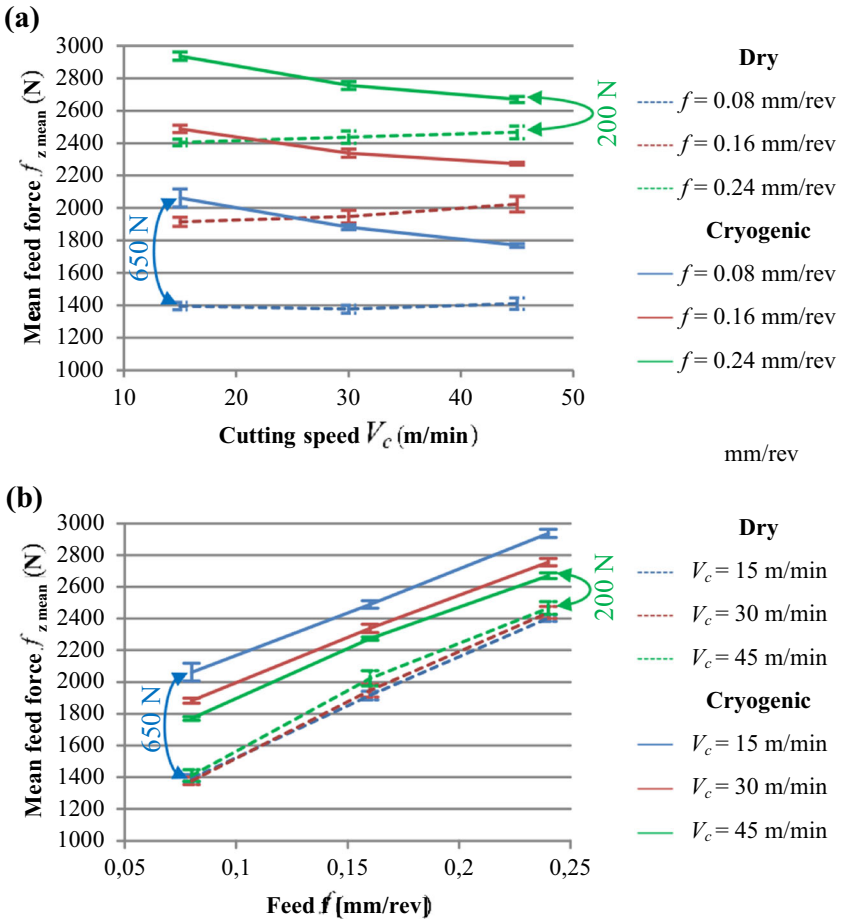

Fig. 6 Mean feed force $F_{z\,mean}$ as a function of **a** cutting speed V_c and **b** feed f

The results show that for the dry-cutting condition, mean feed force $F_{z\,mean}$ increases slightly at higher cutting speeds, whereas it decreases with cryogenic cooling. However, when feed f is increased, it leads to equivalent mean feed force $F_{z\,mean}$ increase in both the cases.

In the case of feed force and for the same set of cutting parameters, the mean value is typically larger than when cryogenic assistance is used. Indeed, the difference ranging from 200 to 650 N represents a change of 10 to 50% more than the values reached under dry-cutting condition. Because the hole shrinkage does not have any effect on the feed force, this can only be explained by the changes in the material properties that are induced by the cooling, making matter removal more difficult.

3.1.3 Evolution of mean torque $M_{z\,mean}$

Figure 7 displays the mean values of torque $M_{z\,mean}$ (measurement explained in Fig. 3) during the drilling as a function of cutting speed V_c and feed f.

The results exhibit that mean torque $M_{z\,mean}$ has a tendency to decrease when the cutting speed becomes higher. This observation is more pronounced under the dry-cutting condition and may be related to an effect of the thermal softening that occurs when the material is heated, leading to a change in the material properties, thus facilitating matter removal. Although this hypothesis is not confirmed here, it is consistent with the increase in the cutting speed. In contrast, a higher feed leads to a larger torque for which the increase is equivalent under both dry and cryogenic-cutting conditions. Irrespective of the cutting parameters, the most noticeable result is that the mean torque is systematically smaller when cryogenic assistance is used. The difference ranging from 0.2 to 2.8 N m corresponds to a torque 3 to 18% weaker than in the dry-cutting case.

To understand the cause of these variations and as explained in Fig. 3, the decomposition of $M_{z\,mean}$ into the contributions of the chip evacuation, margins, and edges is depicted in Fig. 8. It illustrates that the contribution of the edges does not change when cryogenic assistance is used because $M_{z\,edges}$ is the same as for the dry-cutting case. This affirms that the material property changes induced by the cooling have no significant effect on the torque needed to cut the matter. Regarding $M_{z\,margins}$, the extracted values are 22 to 42% smaller than with cryogenic assistance, except for $V_c = 45$ m/min and $f = 0.08$ mm/rev when the value is 5% larger than under the dry-cutting condition. As for $M_{z\,chips}$, the extracted values are mostly smaller with cryogenic assistance, particularly at a low cutting speed ($V_c = 15$ m/min)

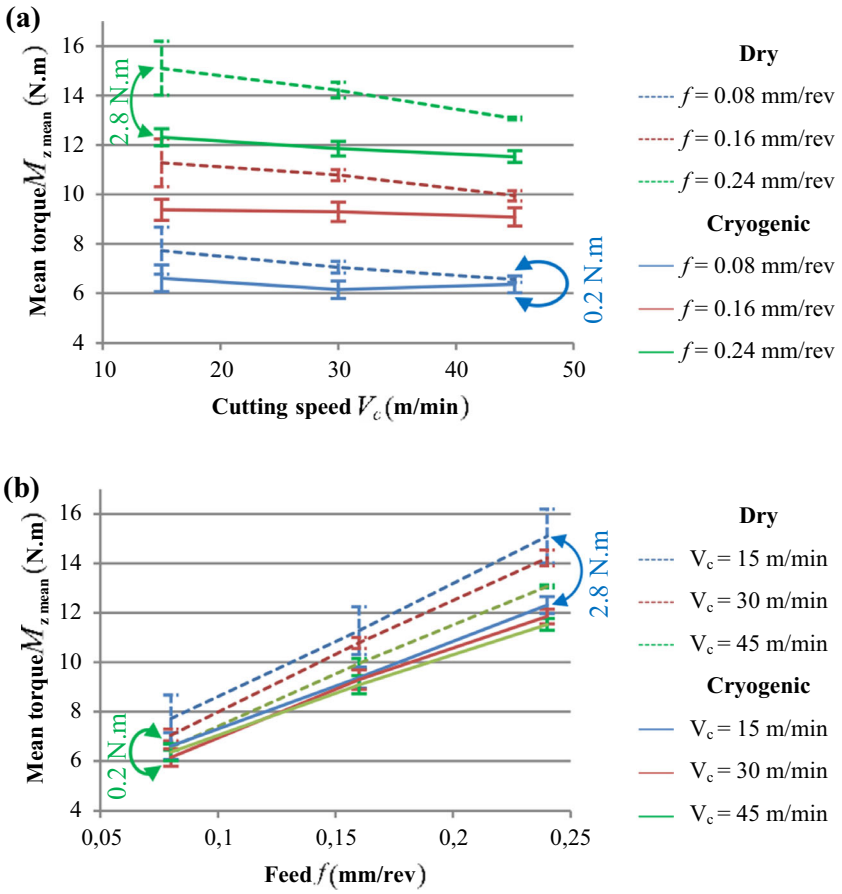

Fig. 7 Mean torque $M_{z\ mean}$ as a function of **a** cutting speed V_c and **b** feed f

when they are 40 to 46% smaller than under the dry-cutting condition. Nevertheless, they are still 25% larger than for set $V_c = 30$ m/min and $f = 0.16$ mm/rev and 30% larger for set $V_c = 45$ m/min and $f = 0.16$ mm/rev. Finally, in every case, except for set $V_c = 45$ m/min and $f = 0.08$ mm/rev, the difference in the mean torque that was highlighted before is explained by the lower contribution of the margins when cryogenic assistance is used. This can be attributed to the fact that the hole shrinkage is significantly reduced under cryogenic assistance, so that the area of contact between the margins and hole is smaller, and thus, the torque induced by the friction is smaller.

3.1.4 Evolution of hole geometry

Figure 9 presents the effect of the cutting speed and feed on the mean shape of the hole for dry and cryogenic drillings, with $Z = 0$ mm being the exit of the hole. These results allow a

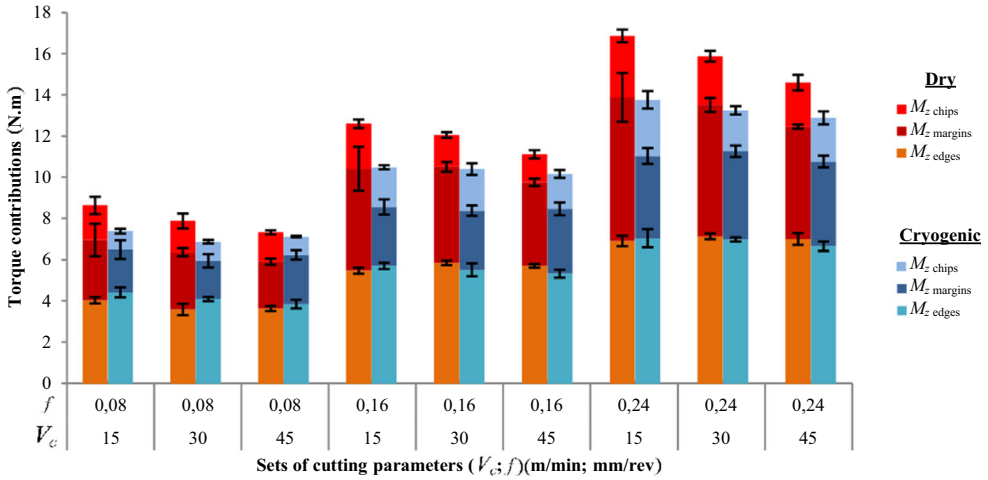

Fig. 8 Torque contributions as a function of cutting speed V_c and feed f

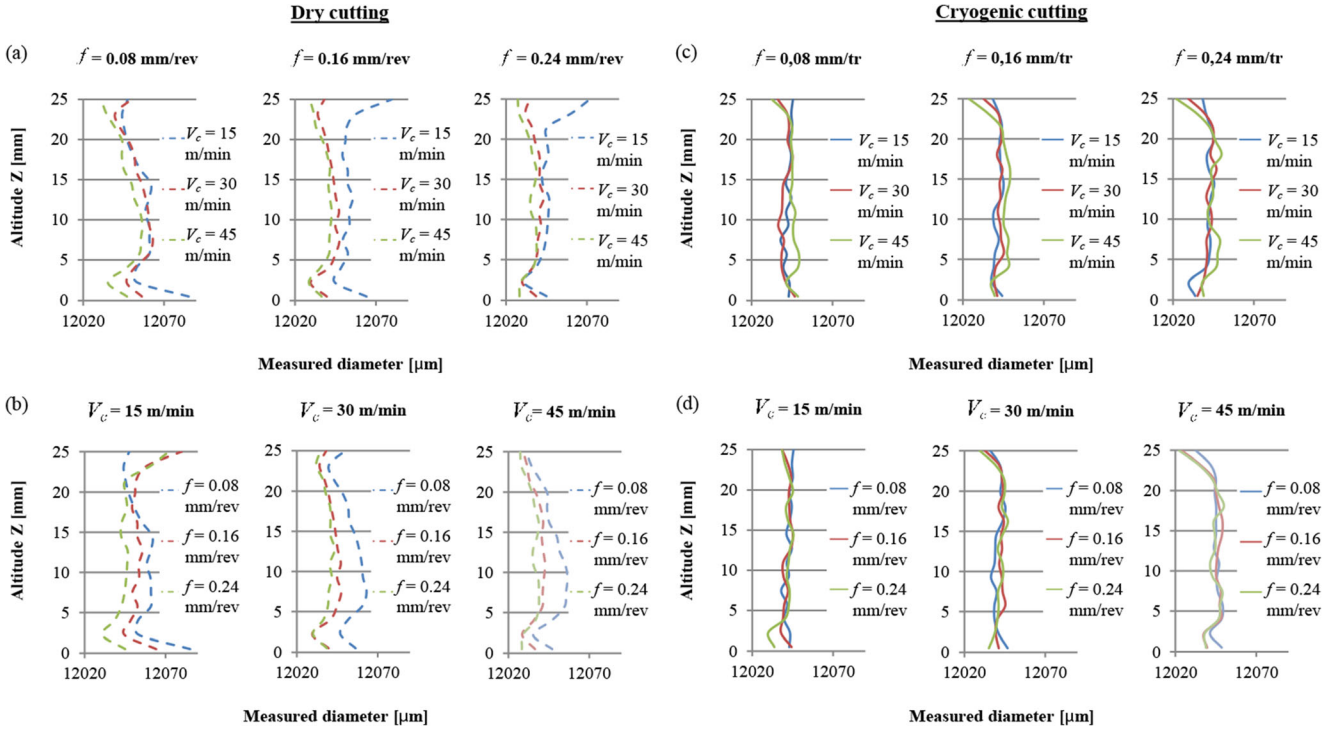

Fig. 9 Mean shape measurements for the holes drilled under the dry-cutting condition as a function of **a** cutting speed V_c and **b** feed f and cryogenic condition as a function of **c** cutting speed V_c and (d) feed f

first qualitative understanding of the effects of the cutting parameters on the shapes of the drilled holes. Particularly, it shows that an increase in V_c or f under the dry-cutting condition leads to a smaller general diameter, with a more obvious effect at the entry of the hole when V_c is increased and in the middle of the hole when f is increased. In contrast, the measurements demonstrate that the shapes of the holes are significantly less affected by the cutting parameter changes when using cryogenic cooling. Nevertheless, increasing the feed still seems to lead to a slight diameter reduction at the entry and exit of the hole, whereas the cutting speed increase only slightly reduces the diameter at the entry.

To quantify the changes in the hole shape explained before, Fig. 10 presents the diameter of the inscribed cylinder of these holes for both cryogenic and dry drilling as a function of the cutting speed and feed. It does not show any clear tendency when cryogenic cooling is applied because the diameters remain rather stable. In the case of dry drilling, however, the diameter of the inscribed cylinder tends to decrease by 10 to 20 µm when either the cutting speed or feed is increased by 15 m/min and 0.08 mm/rev, respectively. This is verified except for the transition between $V_c = 15$ and 30 m/min when $f = 0.08$ and between $f = 0.08$ and 0.16 when $V_c = 15$ m/min. Moreover, these diameters are typically markedly smaller under the dry-cutting condition (up to 40 µm less than with cryogenic assistance), except at a lower cutting speed when they can be equivalent.

Aiming at completing the quantification, Fig. 11 provides the cylindricity of these holes, for both cryogenic and dry drilling, as a function of the cutting speed and feed. Because these values give information of the shape deviation, they remain stable at approximately 100 µm for the cryogenic assistance case and are larger in the case of dry drilling when they can be above 200 µm at a low cutting speed or feed. In addition, an increase in the feed leads to a decrease in the cylindricity, which is also the tendency when the cutting speed is increased but in less significance.

3.2 Phase 2: wear tests

Wear tests were performed for a unique set of cutting parameters ($V_c = 15$ m/min, $f = 0.08$ mm/rev). Breaks of 10-s duration were introduced between each hole to amplify the thermal issues and attain a production pacing. Primarily, this rapid-paced process aimed at identifying the effect of tool wear on the hole shrinkage, cutting forces, and hole dimensions as follows:

- Twenty-two holes were drilled under the dry-cutting condition before the indexable head breaks, ending the process.
- One hundred and twenty-six holes were drilled with cryogenic assistance and long stops were made between the 28th and 29th holes as well as between the 63rd and 126th holes.

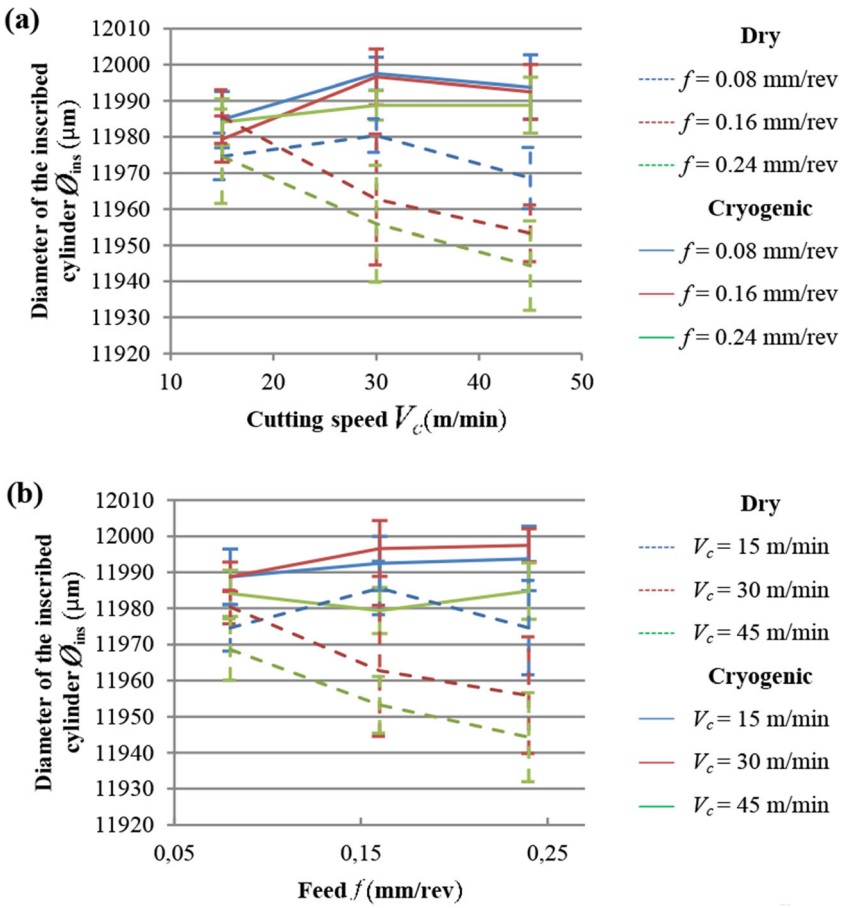

Fig. 10 Diameter of the inscribed cylinder as a function of **a** cutting speed V_c and **b** feed f

Owing to the indexable head rupture under the dry-cutting condition, it was not possible to obtain physical evidence of the wear on the edges or margins of the tool. In the case of cryogenic cutting, there was Ti6Al4V adhesion on the edges and margins, which could have hidden the signs of wear. Consequently, the wear could only be examined through its effects on the hole shrinkage, cutting forces, and hole geometry.

3.2.1 Height of contact *H*

Figure 12 presents the evolution of height of contact H under both dry and cryogenic conditions. With cryogenic assistance, H remains stable at approximately 0.5 mm during the entire process. Under the dry-cutting condition, however, the height of contact significantly increases. Indeed, H is more than quadrupled because it changes from 0.75 mm at the beginning to 4.1 mm at the end of the tests, just before the drill breakage. Because it is already affirmed that the hole shrinkage and heat generation are strongly related, these results can be explained by the heat accumulation caused by the pace of the drillings. Indeed, the shrinkage intensifies during the dry-cutting tests similar to the effect of temperature because no time was given for the drill or sample to cool down. In the case of cryogenic assistance, the temperatures in the cutting zone are limited by the cooling provided by the liquid nitrogen, hence, stabilizing the phenomenon.

3.2.2 Feed force F_z and torque M_z

Figure 13 shows the evolution of mean feed force $F_{z\ mean}$ and mean torque $M_{z\ mean}$ and the margins' contribution to it during the campaign for the dry cutting and cryogenic assistance cases. In both cases, $F_{z\ mean}$ remains quite stable, being approximately 1500 N in the dry cutting case and approximately 2000 N when cryogenic assistance is used. This is expected because it is shown before that the hole shrinkage only affects the torque. Thus, $M_{z\ mean}$ actually increases under the dry-cutting condition, changing from 4.8 to 9.9 N m during the tests, whereas it remains around approximately 7 N m in the cryogenic assistance case. The margins' contribution also increases similar to the mean value for the dry-cutting condition. Consequently, this confirms that the mean torque increases owing to the intensification of the hole shrinkage during the drilling process.

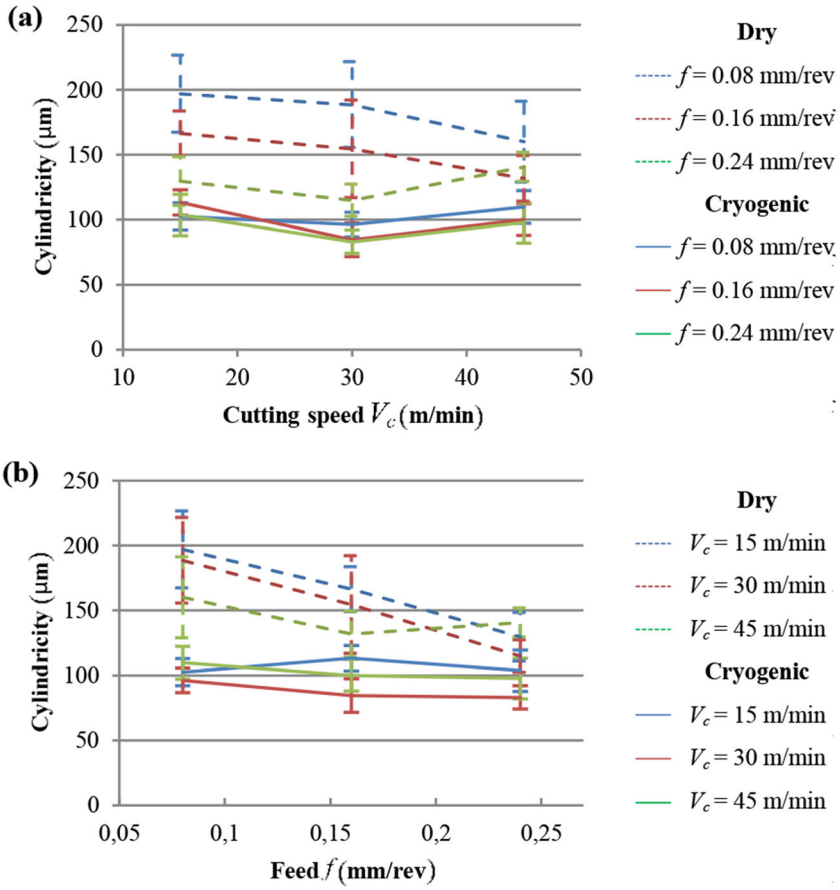

Fig. 11 Cylindricity as a function of cutting speed V_c and feed f

3.2.3 Hole geometry

Figure 14 displays the effect of the number of drillings on the measured shape of the holes, with $Z = 0$ mm being the exit of the hole. Under the dry-cutting condition, for the 22 holes that are machined, an enlargement of the hole is observed at its entry and exit and a progressive decrease in the general diameter during the process is noted. Despite the number of holes drilled with cryogenic assistance being large, the shape of the holes remain stable. Once again, these results are consistent with the fact that hole shrinkage during the operation is amplified by the temperature increase.

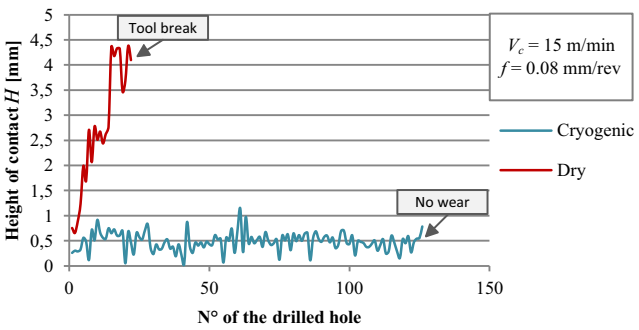

Fig. 12 Evolution of height of contact H during the wear tests

These remarks on the shape were confirmed by the measurements of the diameters of the inscribed cylinder and cylindricity during the wear tests. Indeed, the diameter of the inscribed cylinder remained between 11.950 and 12.000 mm with cryogenic assistance, whereas it decreased from 12.000 to 11.850 mm under the dry-cutting condition. As for cylindricity, it remains at approximately 0.15 mm with cryogenic assistance, whereas it becomes 0.4 mm under the dry-cutting condition after also beginning at approximately 0.15 mm.

4 Conclusions

This work consisted of an experimental investigation of the effects of cryogenic assistance used for the drilling of Ti6Al4V. The first objective was to collect data of the forces and hole dimensions in the cases of dry and cryogenic drilling. The second objective was to relate these results with the phenomenon of hole shrinkage to demonstrate its major role in Ti6Al4V drilling.

The first experimental campaign allowed a first comparison of the dry and cryogenic drilling and provided the trends concerning the effects of cutting speed V_c and feed f. Particularly, it showed that cryogenic cooling reduced the hole shrinkage significantly, ranging from 2.5 to 5.5 times less than

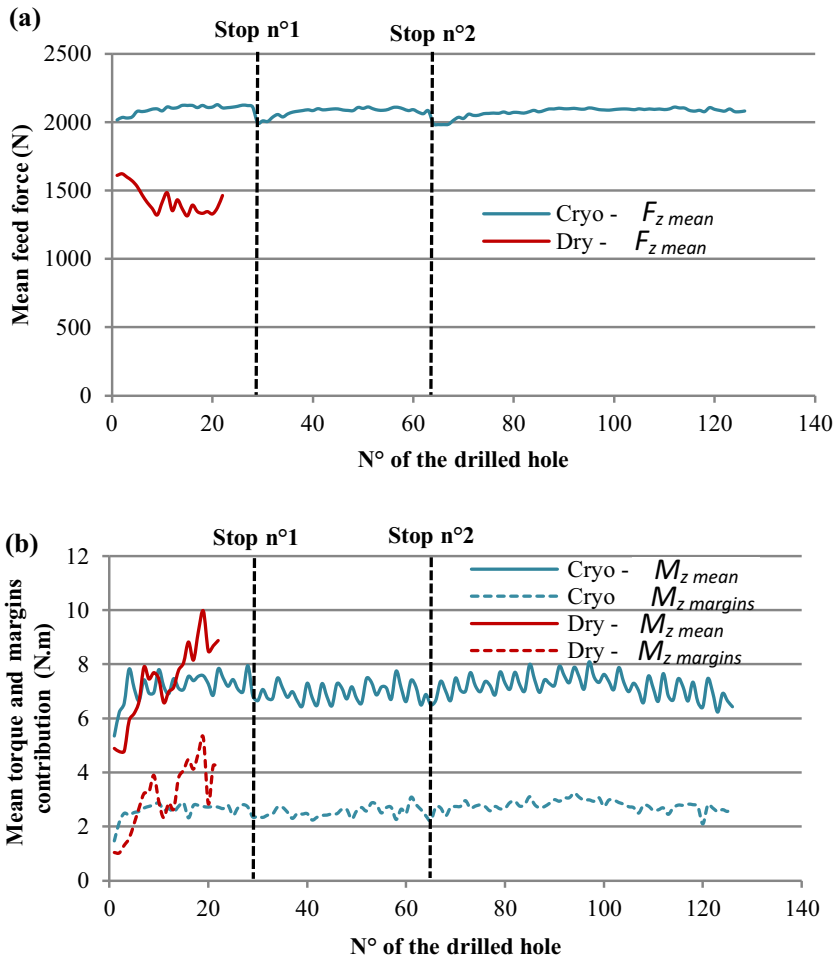

Fig. 13 Evolution of **a** mean feed force $F_{z\,mean}$ and **b** mean torque $M_{z\,mean}$ and margins' contribution during the wear tests

that for dry cutting, thus affirming that the thermal aspect played a key role in this phenomenon.

The consequences of the hole shrinkage limitation on the cutting forces and hole dimensions were highlighted. The close analysis of the torque enabled to decompose the effect of the cutting edges, the margins, and the chip evacuation. Notably, it led to a mean torque $M_{z\,mean}$ reduction owing to a narrower zone of contact between the margins and hole. More importantly, it allowed an approach to better stabilize the hole dimensions when the cutting parameters were modified. These results enable the

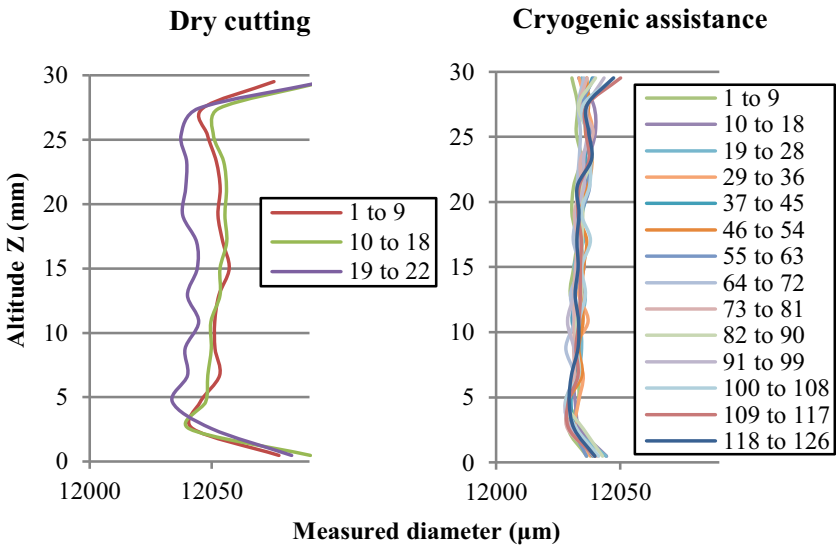

Fig. 14 Measured shape of the holes during the wear tests

design of new drill geometry with reduced margins' width and an increased back tapper angle.

Besides showing the potential of cryogenic assistance in the drilling of Ti6Al4V, the wear tests also exhibited the importance of hole shrinkage. Indeed, the monitoring of the height of contact between the margins and holes displayed that the intensity of the shrinkage escalated rapidly under the dry-cutting condition, leading to larger torques and ultimately to the breaking of the tool after 22 drilled holes. In the case of cryogenic assistance, 126 holes were drilled without any significant changes either in the hole shrinkage or cutting forces. Moreover, the final hole dimensions were gradually reduced in the dry-cutting case, which was consistent with the assessments of the hole shrinkage considering that the hole dimensions remained stable in the cryogenic assistance case.

Finally, this study allowed to bring awareness concerning the phenomenon of hole shrinkage, which seems to be often disregarded in Ti6Al4V drilling. It is the first time that the hole shrinkage is measured in-situ via the height of contact between the margins and the hole and not only from the hole diameter measurement when the workpiece is back at room temperature.

Acknowledgments The Ti6Al4V plates, nitrogen storage/delivery equipment, and machining tools used to perform the drilling tests were supplied by AIRBUS, AIR LIQUIDE, and ISCAR, respectively. Their support is gratefully acknowledged by the authors.

References

1. Donachie MJ (1988) Titanium: a technical guide. ASM International
2. Ghani JA, Che Haron CH, Hamdan SH, Md Said AY, Tomadi SH (2013) Failure mode analysis of carbide cutting tools used for machining titanium alloy. Ceram Int 39:4449–4456. https://doi.org/10.1016/j.ceramint.2012.11.038
3. Ramirez C, Idhil Ismail A, Gendarme C, Dehmas M, Aeby-Gautier E, Poulachon G, Rossi F (2017) Understanding the diffusion wear mechanisms of WC-10%Co carbide tools during dry machining of titanium alloys. Wear 390–391:61–70. https://doi.org/10.1016/j.wear.2017.07.003
4. Cantero JL, Tardío MM, Canteli JA, Marcos M, Miguélez MH (2005) Dry drilling of alloy Ti–6Al–4V. Int J Mach Tools Manuf 45:1246–1255. https://doi.org/10.1016/j.ijmachtools.2005.01.010
5. Dornfeld DA, Kim JS, Dechow H, Hewson J, Chen LJ (1999) Drilling Burr formation in titanium alloy, Ti-6AI-4V. CIRP Ann - Manuf Technol 48:73–76. https://doi.org/10.1016/S0007-8506(07)63134-5
6. Kalidas S, Kapoor SG, DeVor RE (2002) Influence of thermal effects on hole quality in dry drilling, part 1: a thermal model of workpiece temperatures. J Manuf Sci Eng 124:258–266. https://doi.org/10.1115/1.1455645
7. Hong SY, Ding Y (2001) Cooling approaches and cutting temperatures in cryogenic machining of Ti-6Al-4V. Int J Mach Tools Manuf 41:1417–1437. https://doi.org/10.1016/S0890-6955(01)00026-8
8. Dhananchezian M, Pradeep Kumar M (2011) Cryogenic turning of the Ti–6Al–4V alloy with modified cutting tool inserts. Cryogenics 51:34–40. https://doi.org/10.1016/j.cryogenics.2010.10.011
9. Kaynak Y, Gharibi A, Ozkutuk M (2018) Experimental and numerical study of chip formation in orthogonal cutting of Ti-5553 alloy: the influence of cryogenic, MQL, and high pressure coolant supply. Int J Adv Manuf Technol 94:1411–1428. https://doi.org/10.1007/s00170-017-0904-y
10. Venugopal KA, Paul S, Chattopadhyay AB (2007) Tool wear in cryogenic turning of Ti-6Al-4V alloy. Cryogenics 47:12–18. https://doi.org/10.1016/j.cryogenics.2006.08.011
11. Rotella G, Dillon OW, Umbrello D, Settineri L, Jawahir IS (2014) The effects of cooling conditions on surface integrity in machining of Ti6Al4V alloy. Int J Adv Manuf Technol 71:47–55. https://doi.org/10.1007/s00170-013-5477-9
12. Kim DY, Kim DM, Park HW (2018) Predictive cutting force model for a cryogenic machining process incorporating the phase transformation of Ti-6Al-4V. Int J Adv Manuf Technol 1–12:1293–1304. https://doi.org/10.1007/s00170-018-1606-9
13. Pu Z, Outeiro JC, Batista AC, Dillon OW, Puleo DA, Jawahir IS (2012) Enhanced surface integrity of AZ31B Mg alloy by cryogenic machining towards improved functional performance of machined components. Int J Mach Tools Manuf 56:17–27. https://doi.org/10.1016/j.ijmachtools.2011.12.006
14. Pusavec F, Hamdi H, Kopac J, Jawahir IS (2011) Surface integrity in cryogenic machining of nickel based alloy Inconel 718. J Mater Process Technol 211:773–783. https://doi.org/10.1016/j.jmatprotec.2010.12.013
15. Biček M, Dumont F, Courbon C, Pušavec F, Rech J, Kopač J (2012) Cryogenic machining as an alternative turning process of normalized and hardened AISI 52100 bearing steel. J Mater Process Technol 212:2609–2618. https://doi.org/10.1016/j.jmatprotec.2012.07.022
16. Hong SY, Ding Y, Jeong W (2001) Friction and cutting forces in cryogenic machining of Ti–6Al–4V. Int J Mach Tools Manuf 41:2271–2285. https://doi.org/10.1016/S0890-6955(01)00029-3
17. Bermingham MJ, Kirsch J, Sun S, Palanisamy S, Dargusch MS (2011) New observations on tool life, cutting forces and chip morphology in cryogenic machining Ti-6Al-4V. Int J Mach Tools Manuf 51:500–511. https://doi.org/10.1016/j.ijmachtools.2011.02.009
18. Merzouki J, Poulachon G, Rossi F, Ayed Y, Abrivard G (2017) Method of hole shrinkage radial forces measurement in Ti6Al4V drilling. Procedia CIRP, 16th CIRP conference on Modelling of machining operations (16th CIRP CMMO) 58:629–634. https://doi.org/10.1016/j.procir.2017.03.226
19. Li R, Riester L, Watkins T, Blau P, Shih A (2007) Metallurgical analysis and nanoindentation characterization of Ti–6Al–4V workpiece and chips in high-throughput drilling. Mater Sci Eng A 472:115–124. https://doi.org/10.1016/j.msea.2007.03.054
20. Yagishita H, Morita Y (2018) Effect of phase transformation upon hole making accuracy of Ti6Al4V by orbital drilling. Procedia Manuf 26:152–163. https://doi.org/10.1016/j.promfg.2018.07.022
21. Bono M, Ni J (2001) The effects of thermal distortions on the diameter and cylindricity of dry drilled holes. Int J Mach Tools Manuf 41:2261–2270. https://doi.org/10.1016/S0890-6955(01)00047-5
22. Bonnet C (2010) Compréhension des mécanismes de coupe lors du perçage à sec de l'empilage Ti6Al4V/Composite fibre de carbone. Dissertation, Arts et Métiers ParisTech
23. Nobre JP, Outeiro JC (2015) Evaluating residual stresses induced by drilling of Ti-6Al-4V alloy by using an experimental-numerical methodology. Procedia CIRP, 15th CIRP conference on modelling of machining operations (15th CMMO) 31:215–220. https://doi.org/10.1016/j.procir.2015.03.062